# Supporting information

## Kinetic characterization of neuraminic acid synthases and evaluation of their application potential

Mehmet Mervan Çakar[a], Nevena Milčić[a], Theofania Andreadaki[b], Simon Charnock[b], Wolf-Dieter Fessner[c], Zvjezdana Findrik Blažević[a,*]

[a] University of Zagreb Faculty of Chemical Engineering and Technology, Trg Marka Marulića 19, 10000, Zagreb, Croatia

[b] Prozomix Limited, Station Court, Haltwhistle, Northumberland, NE49 9HN, UK

[c] Technical University of Darmstadt, Institute of Organic Chemistry and Biochemistry, Peter-Grünberg-Strasse 4, 64287 Darmstadt, Germany

*author for correspondence, zfindrik@fkit.unizg.hr, zfindrik@fkit.hr

### Table of contents

## SI 1. Reaction scheme.

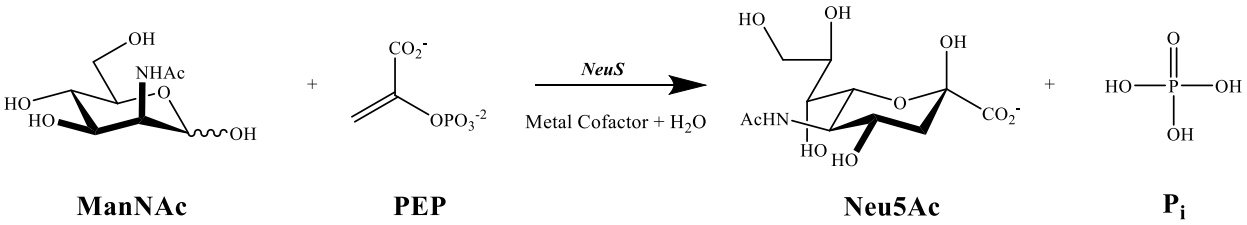


**ManNAc** **PEP** **Neu5Ac** **$P_i$**

**Scheme 1.** Synthesis of Neu5Ac via aldol-like condensation of ManNAc and PEP.

## SI 2. Previously estimated kinetic constants for neuraminic acid synthases in the literature.

**Table S1.** Biochemical features of NeuS enzymes from different organisms in the synthesis of *N*-acetylneuraminic acid.

| Organism | $K_m^{ManNAc}$ [mM] | $V_m^{ManNAc}$ [U mg$^{-1}$] | $K_m^{PEP}$ [mM] | $k_{cat}^{ManNAc}$ [min$^{-1}$] | $k_{cat}^{PEP}$ [min$^{-1}$] | $K_i$ [mM] | pH Range; [Optimum] | Temperature Range; [Optimum] [°C] | Metal Preference | Molecular weight [kDA] | Reference |
|---|---|---|---|---|---|---|---|---|---|---|---|
| ***N. meningitidis*** | - | | 0.16 | - | - | 0.0031* | - | - | $Mn^{2+}$; (1 mM) | | (Liu et al. 2009) |
| | 11.6 | | - | 49.8 | - | | 7-10; [7.5] | 10-70; [37] | $Co^{2+}$, $Mn^{2+}$, $Mg^{2+}$; (1 mM) | | (Hao et al. 2005) |
| | 9.4 | | 0.25 | - | 54 | | [7.5] | - | $Mn^{2+}$; (1 mM) | | (Gunawan et al. 2005) |
| | 6.3 | 6.74 | 0.04 | - | - | | 6.5-10; [8.3] | - | $Mn^{2+}$ (0.5 mM), $Mg^{2+}$ (2 mM) | | (Blacklow and Warren 1962) |
| ***C. jejuni*** | 17.6 | | 7.30 | 19.9 | 19 | | - | - | $Co^{2+}$, $Mn^{2+}$, $Mg^{2+}$; (0.1 mM) | 74 (dimer) | (Linton et al. 2000; Sundaram et al. 2004) |
| ***A. salmonicida*** | 333 | | 0.06 | 22.5 | 19.9 | | 7.5-10; [8.0] | 5-60; [45] | $Co^{2+}$, $Mn^{2+}$, $Mg^{2+}$; (5 mM) | | (Gurung et al. 2013) |
| ***S. agalactiae*** | - | | - | - | - | | 5-10; [7.0] | 37 | $Co^{2+}$, $Mn^{2+}$, $Mg^{2+}$; (1 mM) | 78 (dimer) | (Suryanti et al. 2003) |
| ***E. coli* K1** | - | 0.00044 | - | - | - | | 8.0 | 15-60; [45] | $Mn^{2+}$, $Mg^{2+}$; (8.3 mM) | | (Vann et al. 1997) |

| | | | | | | | | | | | |
|---|---|---|---|---|---|---|---|---|---|---|---|
| ***E. coli*** | | | | | | | | | | 160 (tetramer) | |
| ***M. viscosa*** | 18 ± 5 | | 0.8 ± 0.2 | 223 | 225 | | 7-10; [7.3] | 5-55; [30] | $Co^{2+}$ (0.01 mM), $Mn^{2+}$ (2 mM), $Mg^{2+}$ (2 mM) | | (Berg et al. 2015) |
| ***E. coli* K1-M12** | 5.6 | 0.487 | 0.04 | - | - | | 7.5 | 20-60; [35] | $Mn^{2+}$, $Ca^{2+}$; (1 mM) | 52 (dimer) | (Komaki et al. 1997) |
| ***I. loihiensis*** | 11 ± 0.2 | 0.066 | 1.2 ± 0.3 | 132 | 132.5 | | 5.5-9.5; [7.0] | 20-55; [40] | $Mn^{2+}$ (1 mM) | 95 (dimer) | (García García et al. 2015) |
| *****Methyl 5-Acetamido-3,5-dideoxy-2-methylidine-4,6,7,8,9-penta-O-acetyl-D-glycero-D-galacto-2-nonulosonate | | | | | | | | | | | |

## SI 3 Determination of concentrations of compounds by HPLC – chromatograms and calibration curves

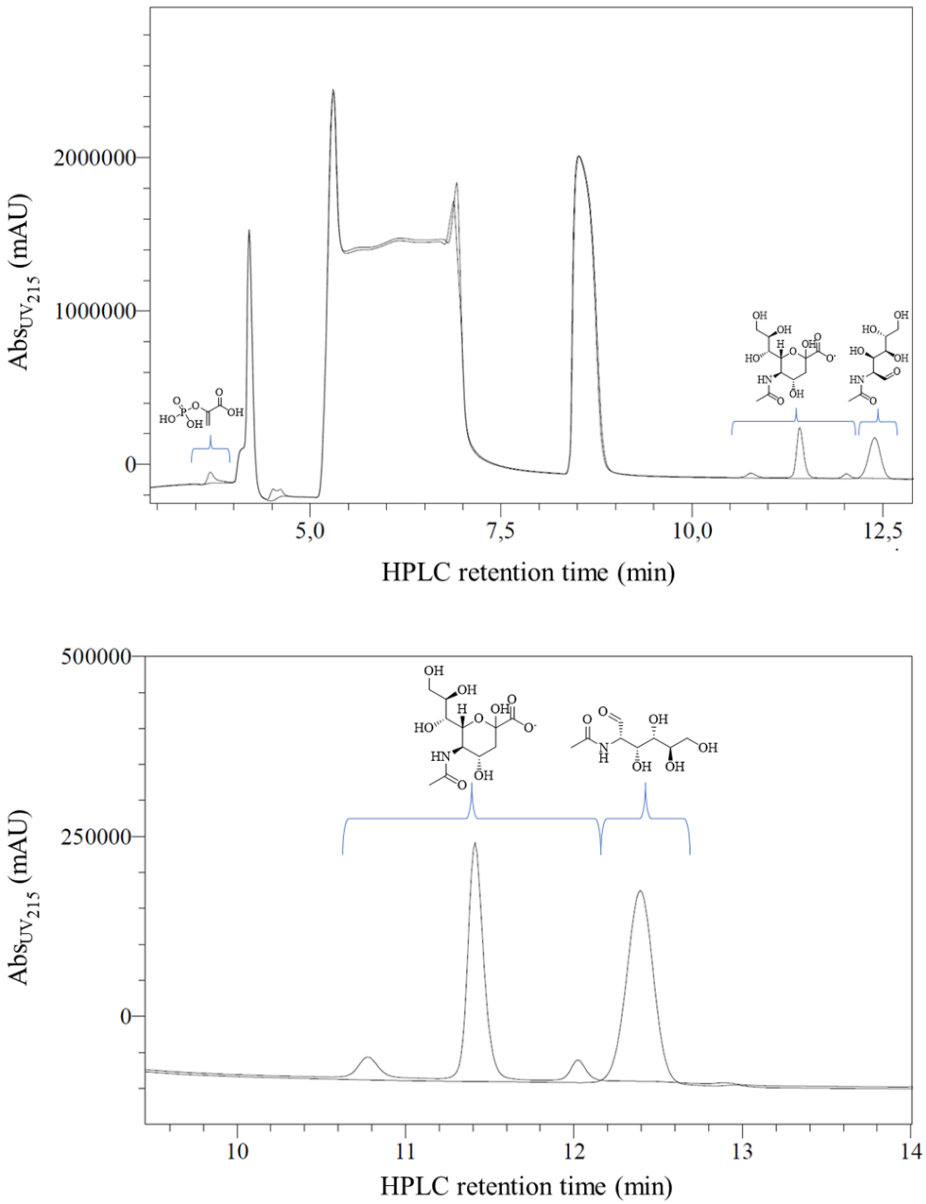


**Figure S1**. HPLC chromatogram of Neu5Ac and ManNAc peaks detected by PDA detector with retention times of 11.4 and 12.4 min, respectively.

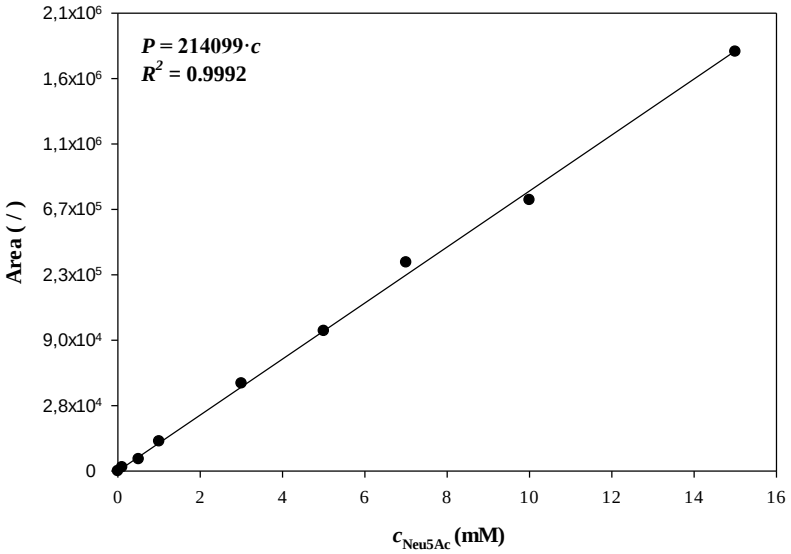


**Figure S2**. Calibration curve of Neu5Ac

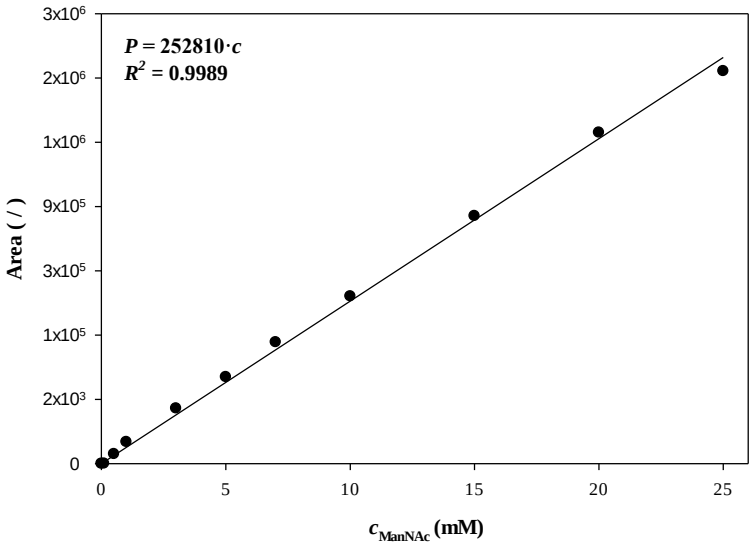


**Figure S3**. Calibration curve of ManNAc

## SI 4 Multiple sequence alignment of different bacterial NeuS amino acid sequences.

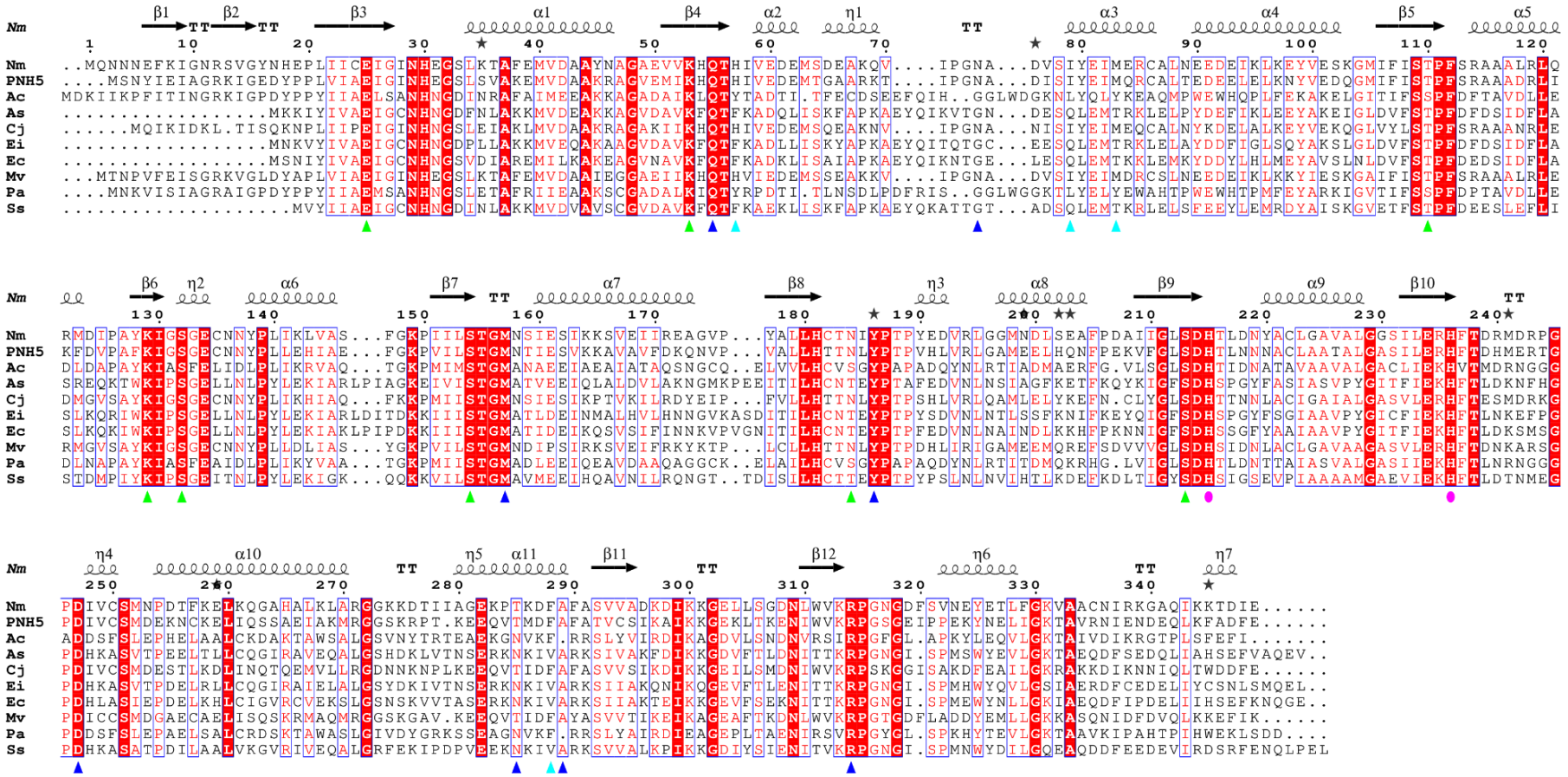


**Figure S4** Multiple sequence alignment of different bacterial NeuS amino acid sequences. The secondary structure elements indicated above the alignment belonging to *N. meningitidis* NeuS. Identical residues are indicated as white letters on a red background, and residues with similar properties as red letters in blue boxes. Positions interacting with PEP, ManNAc, acetyl and metal ions are indicated with green, blue, cyan and pink coloured symbols. Sequences are from *N. meningitidis*, $PNH_5$, *A. caviae*, *A. salmonicida*, *C. jejuni*, *E. ictalurid*, *E. coli*, *M. viscosa*, *P. aeruginosa*, and *Streptococcus* sp.

## SI 5 The effect of different buffers on *Nm*NeuS activity

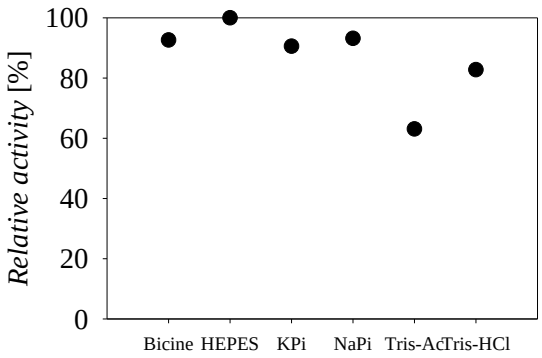


**Figure S5.** Effect of buffer on *Nm*NeuS activity ($c_{ManNAc}$ = 5 mM, $c_{PEP}$ = 5 mM, $c_{Mn^{2+}}$= 1 mM, $\gamma_{NeuS}$ = 0.0125 mg mL$^{-1}$, 150 mM buffers, pH 7.6, 37 °C, 100% relative activity corresponds to 9.12 U mg$^{-1}$).

## SI 6 Analysis of metal removal efficiency from the enzyme structure

**Table S2** IPC MS analysis before and after the metal removal by EDTA treatment.

| Enzyme | | before [mg $kg^{-1}$] | after [mg $kg^{-1}$] |
|---|---|---|---|
| *Nm*NeuS | $Ni^{2+}$ | 0.69 A1 | <0.05 |
| | $Mn^{2+}$ | <0.05 A1 | <0.05 |
| $PNH_5$ | $Ni^{2+}$ | 1.16 A2 | <0.05 |
| | $Mn^{2+}$ | <0.05 A2 | <0.05 |

## SI 7 $PNH_5$ stability at pH 7.5

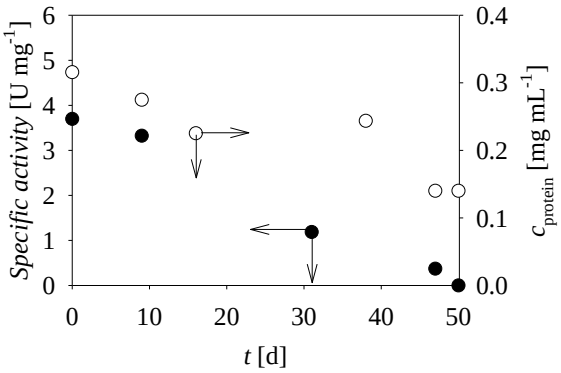


**Figure S6.** Storage stability presented as the change of specific activity and protein concentration during 50 days for $PNH_5$ (150 mM sodium phosphate buffer, pH 7.5, $c_{ManNAc}$ = 20 mM, $c_{PEP}$ = 20 mM, $c_{Co}^{2+}$= 0.05 mM, $\gamma_{PNH5}$ = 0.048, 37 °C).

## SI 8 Particle size distribution for $PNH_5$ in solution of soluble proteins after 61 days of incubation

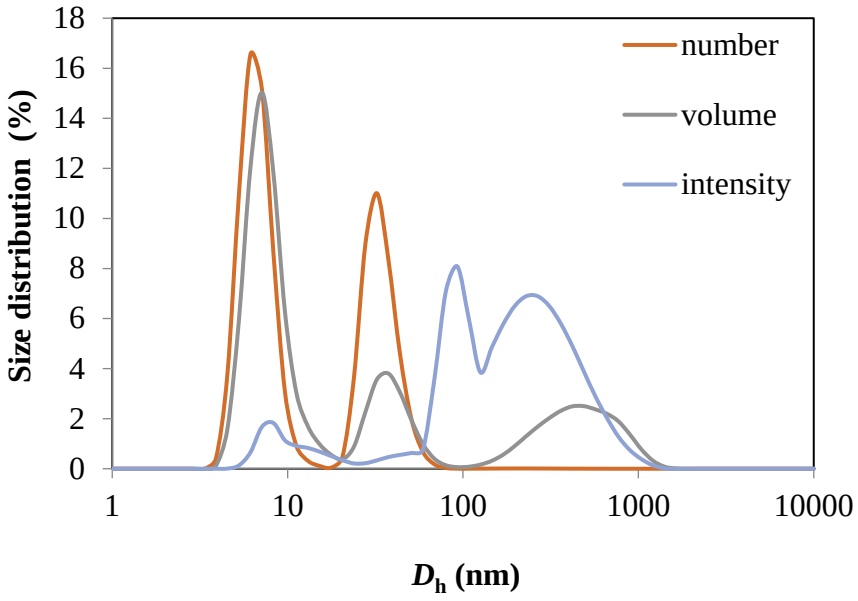


**Figure S7**. PSD of $PNH_5$ after 61 days of incubation and centrifugation.

## SI 9 Mathematical model validation

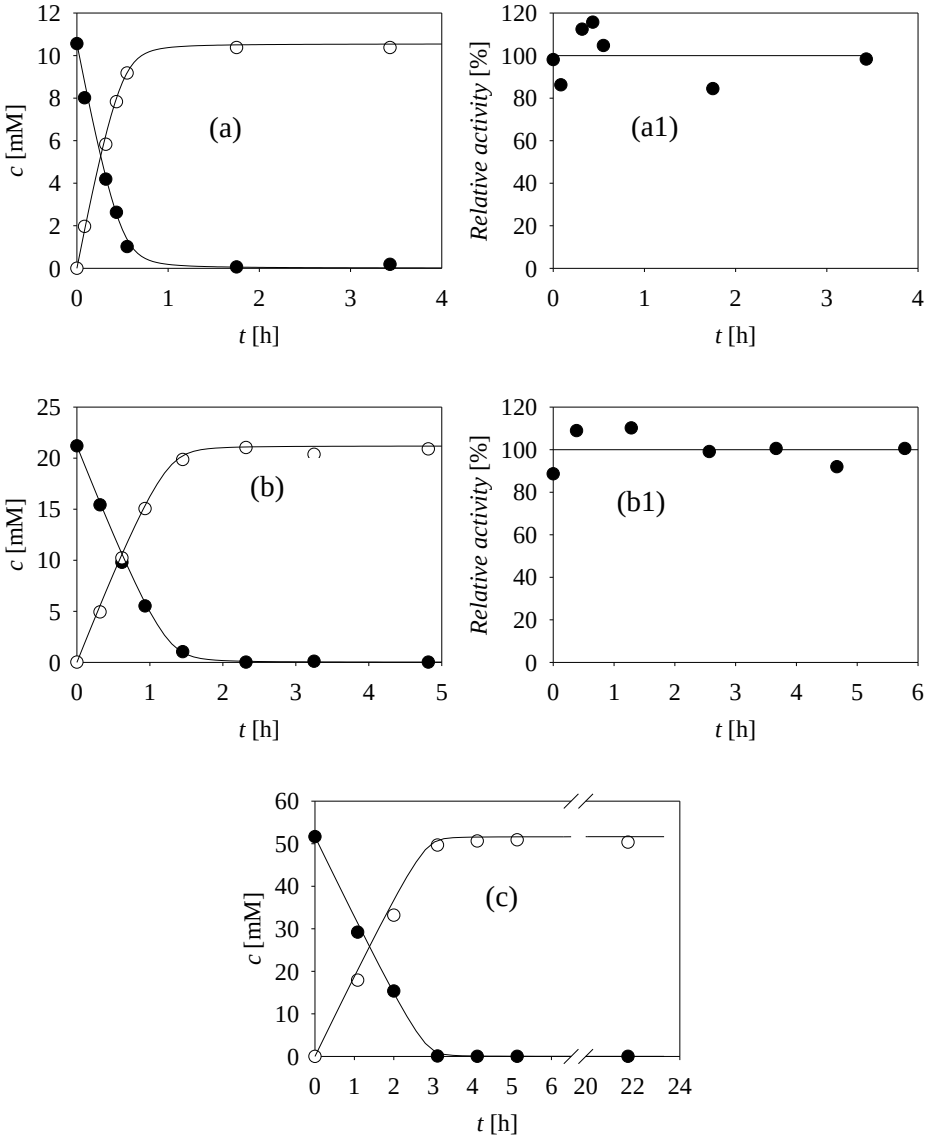


**Figure S8** Synthesis of Neu5Ac catalysed by *Nm*NeuS in the batch reactor at different reaction conditions (150 mM sodium phosphate buffer pH 7.5, 37 °C, $\gamma_{NeuS}$ = 0.021 mg mL$^{-1}$, $c_{Co2+}$= 0.05 mM). **(a)**. $c_{ManNAc}$ = 11.53 mM, $c_{PEP}$= 12 mM. **(a1)** Operational stability of *Nm*NeuS during the experiment presented in A. **B**. $c_{ManNAc}$ = 21.20 mM, $c_{PEP}$ = 22.00 mM. **(b1)**. Operational stability of *Nm*NeuS during the experiment presented in B. **(c)**. $c_{ManNAc}$ = 51.66 mM, $c_{PEP}$ = 50.00 mM. **(d)**. $c_{ManNAc}$ = 83.79 mM, $c_{PEP}$ = 100.00 mM. Legend: **(a) - (c)** black circles – ManNAc, white circles – Neu5Ac, black line – simulation. **(a1) - (c1)** – black circles – relative activity of *Nm*NeuS during the experiments, black line – model simulation.

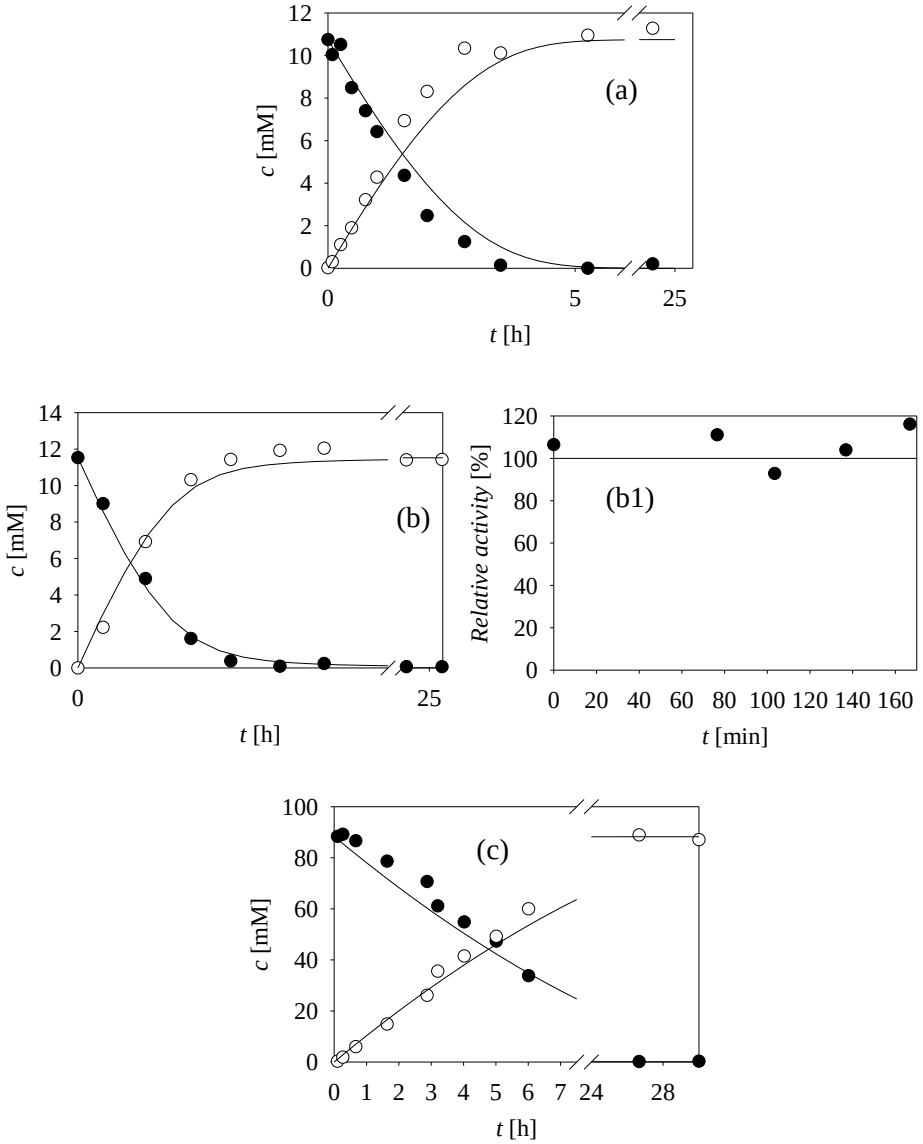


**Figure S9** Synthesis of Neu5Ac catalysed by $PNH_5$ in the batch reactor at different reaction conditions (150 mM sodium acetate buffer pH 5.5, 37 °C, $\gamma_{PNH5}$ = 0.053 mg $mL^{-1}$, $c_{Co2+}$= 0.05 mM). **(a)**. $c_{ManNAc}$ = 11.53 mM, $c_{PEP}$ = 11.05 mM. **(b)**. $c_{ManNAc}$ = 11.91 mM, $c_{PEP}$= 12.00 mM. **(b1)**. Operational stability of $PNH_5$ during the experiment presented in B. **(c)**. $c_{ManNAc}$ = 88.38 mM, $c_{PEP}$= 100.00 mM. Legend: (a) – (c) black circles – ManNAc, white circles – Neu5Ac, black line – simulation. (b1) – black circles – relative activity of $PNH_5$ during the experiments, black line – model simulation.

**Table S3** Statistical output of the mathematical model.

| ***Nm*NeuS** | | | | | |
|---|---|---|---|---|---|
| **Fig.** | **Standard deviation of data** | **$R^2$** | **Coeff. of determination** | **Correlation** | **MSC** |
| **S8A** | 0.280540329 | 0.998295099 | 0.995505068 | 0.998473402 | 5.26194770 |
| **S8B** | 0.359365218 | 0.999344970 | 0.998454494 | 0.999579548 | 6.37240376 |
| **S8C** | 1.46336994 | 0.998185015 | 0.995806452 | 0.998918997 | 5.33135102 |
| **10A** | 4.77148538 | 0.992289507 | 0.971853404 | 0.987998042 | 3.47032886 |
| **$PNH_5$** | | | | | |
| **S9A** | 0.418627481 | 0.997240415 | 0.993522952 | 0.997738874 | 4.92837926 |
| **S9B** | 2.70752541 | 0.968398642 | 0.919882547 | 0.959145400 | 2.41315045 |
| **S9C** | 1.39119768 | 0.997823137 | 0.993593984 | 0.997148425 | 4.95960866 |
| **10B** | 4.63256986 | 0.993310182 | 0.978845053 | 0.990664014 | 3.76497241 |

Explanation of the meaning of the statistical output presented in Table S3 (García García et al. 2015)

**R-squared** is defined by the formula:

$$R^2 = \frac{\left| \sum_{i=1}^{n} w_i \cdot {Y_{obs_i}}^2 - \sum_{i=1}^{n} w_i \left( Y_{obs_i} - Y_{cal_i} \right)^2 \right|}{\sum_{i=1}^{n} w_i \cdot {Y_{obs_i}}^2}$$

where $n$ is the number of points and $w_i$ are the weights applied to each point. The expression is similar to that of the coefficient of determination, with the sum of the squares of the observed values occupying a similar position to that of the variance in the coefficient of determination formula.

The **coefficient of determination** is defined by the formula:

$$\text{Coefficient of determination} = \frac{\sum_{i=1}^{n} w_i \left( Y_{obs_i} - \overline{Y}_{obs} \right)^2 - \sum_{i=1}^{n} w_i \left( Y_{obs_i} - Y_{cal_i} \right)^2}{\sum_{i=1}^{n} w_i \left( Y_{obs_i} - \overline{Y}_{obs} \right)^2}$$

where $n$ is the number of points, $w_i$ are the weights applied to each point and $\overline{Y_{obs}}$ is the weighted mean of the observed data. The coefficient of determination is a measure of the fraction of the total variance accounted for by the model and is an appropriate measure of the goodness-of-fit.

The **correlation** between two variables $X$ and $Y$ is defined by the expression:

$$\text{Correlation} = \frac{\sum_{i=1}^{n} w_i \left( x_i - \overline{x} \right) \left( y_i - \overline{y} \right)}{\sqrt{\sum_{i=1}^{n} w_i \left( x_i - \overline{x} \right)^2} \sqrt{\sum_{i=1}^{n} w_i \left( y_i - \overline{y} \right)^2}}$$

where $\overline{x}$ and $\overline{y}$ are the weighted means of $X$ and $Y$, n is the number of points, and wi are the weights applied to the points. This may be interpreted as an indication on how the changes in one variable are correlated with changes in the other. The value reported by SCIENTIST is the correlation between observed and calculated values of the dependent variables.

**Model Selection Criterion (MSC)** is defined by the following expression:

$$MSC = \ln\left(\frac{\sum_{i=1}^{n} w_i \left(Y_{obs_i} - \overline{Y}_{obs}\right)^2}{\sum_{i=1}^{n} w_i \left(Y_{obs_i} - \overline{Y}_{cal_i}\right)^2}\right) - \frac{2p}{n}$$

It is based on the modified Akaike Information Criterion (AIC). The original AIC is dependent on the magnitude of the data points, as well as the number of observations. The most appropriate model according to AIC is the one with the smallest value of AIC. SCIENTIST uses a modified AIC called MSC. The most appropriate model will be the one with the largest MSC.

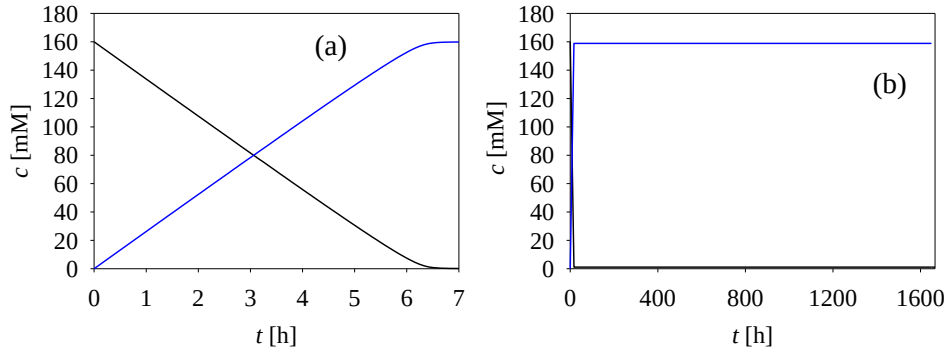


**Figure S10** Simulation of the synthesis of Neu5Ac catalysed by *Nm*NeuS in **(a)**. batch reactor ($c_{ManNAc}$ = 160 mM, $c_{PEP}$= 160 mM, $\gamma_{NmNeuS}$ = 0.028 mg mL$^{-1}$, $c_{Co^{2+}}$= 0.05 mM) and **(b)**. continuous stirred tank reactor ($c_{ManNAc}$ = 160 mM, $c_{PEP}$= 160 mM, $\gamma_{NmNeuS}$ = 0.28 mg mL$^{-1}$, $c_{Co^{2+}}$= 0.05 mM, $\tau$ = 150 min).

## References


Berg TO, Gurung MK, Altermark B, Smalås AO, Ræder ILU (2015) Characterization of the N-acetylneuraminic acid synthase (NeuB) from the psychrophilic fish pathogen *Moritella viscosa*. Carbohydr Res 402:133–145

Blacklow RS, Warren L (1962) Biosynthesis of sialic acids by *Neisseria meningitidis*. J Biol Chem 237:3520–3526. https://doi.org/10.1016/s0021-9258(19)70850-3

García García MI, Lau K, Von Itzstein M, García Carmona F, Sánchez Ferrer Á (2015) Molecular characterization of a new N-acetylneuraminate synthase (NeuB1) from *Idiomarina loihiensis*. Glycobiology 25:115–123. https://doi.org/10.1093/glycob/cwu096

Gunawan J, Simard D, Gilbert M, Lovering AL, Wakarchuk WW, Tanner ME, Strynadka NCJ (2005) Structural and mechanistic analysis of sialic acid synthase NeuB from *Neisseria meningitidis* in complex with $Mn^{2+}$, phosphoenolpyruvate, and N-acetylmannosaminitol. J Biol Chem 280:3555–3563. https://doi.org/10.1074/jbc.M411942200

Gurung MK, Ræder IL, Altermark B, Smalås AO (2013) Characterization of the sialic acid synthase from *Aliivibrio salmonicida* suggests a novel pathway for bacterial synthesis of 7-O-acetylated sialic acids. Glycobiology 23:806–819. https://doi.org/10.1093/glycob/cwt018

Hao J, Balagurumoorthy P, Sarilla S, Sundaramoorthy M (2005) Cloning, expression, and characterization of sialic acid synthases. Biochem Biophys Res Comm 338:1507–1514. https://doi.org/10.1016/j.bbrc.2005.10.113

Komaki E, Otha Y, Tsukada Y (1997) Purification and characterization of N-acetylneuraminate synthase from *Escherichia coli* Kl-M12. Biosci Biotechnol Biochem 61:2046–2050. https://doi.org/10.1271/bbb.61.2046

Linton D, Karlyshev AV, Hitchen PG, Morris HR, Dell A, Gregson NA, Wren BW (2000) Multiple N-acetyl neuraminic acid synthetase (neuB) genes in *Campylobacter jejuni*: Identification and characterization of the gene involved in sialylation of lipo-oligosaccharide. Mol Microbiol 35:1120–1134. https://doi.org/10.1046/j.1365-2958.2000.01780.x

Liu F, Lee HJ, Strynadka NCJ, Tanner ME (2009) Inhibition of *Neisseria meningitidis* sialic acid synthase by a tetrahedral intermediate analogue. Biochemistry 48:9194–9201. https://doi.org/10.1021/bi9012758

Sundaram AK, Pitts L, Muhammad K, Wu J, Betenbaugh M, Woodard RW, Vann WF (2004) Characterization of N-acetylneuraminic acid synthase isoenzyme 1 from *Campylobacter jejuni*. Biochem J 383:83–89. https://doi.org/10.1042/BJ20040218

Suryanti V, Nelson A, Berry A (2003) Cloning, over-expression, purification, and characterisation of N-acetylneuraminate synthase from *Streptococcus agalactiae*. Prot Expr Purif 27:346–356. https://doi.org/10.1016/S1046-5928(02)00633-2

Vann WF, Tavarez JJ, Crowley J, Vimr E, Silver RP (1997) Purification and characterization of the *Escherichia coli* K1 *neuB* gene product N-acetylneuraminic acid synthetase. Glycobiology 7:697–701. https://doi.org/10.1093/glycob/7.5.697